Metallophysics and Advanced Technologies
Металофіз. новітні технол.
Metallofiz. Noveishie Tekhnol.
2022, vol. 44, No. 9, pp. 1179–1193
https://doi.org/10.15407/mfint.44.09.1179
Reprints available directly from the publisher

PACS numbers: 61.46.-w, 72.80.Tm, 75.50.Gg, 75.75.+a, 77.22.Ch, 81.07.Bc

Electrical and Magnetic Properties of Polymeric Nanocomposites Based on Nickel Ferrites Modified by Copper Sulphide

R. V. Mazurenko, S. L. Prokopenko, G. M. Gunja, L. P. Storozhuk, S. M. Makhno, and P. P. Gorbyk

O. O. Chuiko Institute of Surface Chemistry, N.A.S. of Ukraine,
17 General Naumov Str.,
UA-03164 Kyiv, Ukraine

Nanosize nickel ferrite was synthesized by the sol–gel autocombustion method. The surface of nickel ferrite was modified by copper sulphide with the volume fractions from 0.2 to 0.42. For the $CuS/NiFe_2O_4$ composites the values of complex permittivity and permeability in the microwave range, values of conductivity at low frequencies and magnetic characteristics were investigated. Polymer composites $CuS/NiFe_2O_4$–polychlorotrifluoroethylene (PCTFE) were obtained by hot pressing technique. With an increase in the content of copper sulphide of polymer composites, an increase in the values of the complex dielectric constant in the microwave range of 2–3 times was observed. The values of electrical conductivity for the $0.2CuS/NiFe_2O_4$–PCTFE system are 4–5 orders of magnitude lower than for the $0.42CuS/NiFe_2O_4$–PCTFE system with an increase in the concentration of copper sulphide in polymer composites. The change in the ratio of the conducting and magnetic components in the studied system makes it possible composites with adjustable permittivity and permeability in the microwave range.

Key words: polymer nanocomposite, nickel ferrite, copper sulphide, complex permittivity, complex permeability, specific magnetization.

Методою золь–ґель-автогоріння синтезовано нанорозмірний ніклевий ферит. Було проведено модифікування поверхні ніклевого фериту сульфідом міді з об'ємним вмістом від 0,2 до 0,42. Для композитів $CuS/NiFe_2O_4$ досліджено комплексну діелектричну та магнетну проник-

Corresponding author: Ruslana V. Mazurenko
E-mail: r.v.mazurenko@gmail.com

Citation: R. V. Mazurenko, S. L. Prokopenko, G. M. Gunja, L. P. Storozhuk, S. M. Makhno, and P. P. Gorbyk, Electrical and Magnetic Properties of Polymeric Nanocomposites Based on Nickel Ferrites Modified by Copper Sulphide, *Metallofiz. Noveishie Tekhnol.*, **44**, No. 9: 1179–1193 (2022). DOI: 10.15407/mfint.44.09.1179

ності в надвисокочастотному діяпазоні, електропровідність на низьких частотах та магнетні характеристики. Методою гарячого пресування одержано полімерні композити $CuS/NiFe_2O_4$–поліхлортрифторетилен (ПХТФЕ). При збільшенні вмісту сульфіду міді в полімерних композитах спостерігалось збільшення в 2–3 рази значень комплексної діелектричної проникности в НВЧ діяпазоні. Значення електропровідности для системи $CuS/NiFe_2O_4$–ПХТФЕ на 4–5 порядків величини нижчі, ніж для системи $CuS/NiFe_2O_4$–ПХТФЕ із збільшенням вмісту сульфіду міді в полімерних композитах. Зміна співвідношення провідної та магнетної складових у досліджуваній системі дає змогу створювати композити з реґульованою діелектричною та магнетною проникностями в надвисокочастотному діяпазоні.

Ключові слова: полімерний нанокомпозит, ферит ніклю, сульфід міді, комплексна діелектрична проникність, комплексна магнетна проникність, питома намагнетованість.

(Received December 16, 2021; in final version, August 4, 2022)

1. INTRODUCTION

The interaction of nanomaterials with an electromagnetic (EM) wave has been of great interest for many years [1, 2]. The using of electronic and microelectronic devices has a negative impact on work electronic equipment and human body. It causes the necessity for effective electromagnetic interference shielding. Particular interest is focused on absorption in the microwave range, since the number of new sources in this range is increasing (mobile and satellite communications, radar, wireless networks, *etc*.).

The creation of coatings with controlled electrophysical characteristics based on structures with nanoscale cluster and dispersed components is necessary for effective absorption of an electromagnetic wave. The absorption of coatings at one frequency or in a certain frequency range depends on an optimal combination of dielectric, magnetic properties, thickness of absorbing layers, and their impedance and attenuation coefficient. Absorbing coatings can work on the principle of interference, scattering of EM waves, absorption of electromagnetic energy. Often, different principles are combined to create absorbing electromagnetic coatings [3, 4]. Such coatings can be created based on ferrites (characterized by high magnetic losses), complex organic compounds, carbon and semiconductor materials. In particular, nanostructured spinel ferrites with the formula $MeFe_2O_4$ (where $Me = Co^{2+}$, Ni^{2+}, Fe^{2+}, Zn^{2+}, Cu^{2+} *etc*.) can be obtained of various structures, shapes, sizes by changing their chemical composition (which leads to the occurrence of multiple dielectric and magnetic resonances [5]) in order to select the necessary magnetic properties [6, 7].

For intensification of the EM wave adsorption use of magnetic nanoparticles modified at the interface by conductive components (carbon and semiconductor materials, metallic particles, conductive polymers *etc.* [4, 8–11].

Copper sulphide (CuS), a type of semiconductor transition-metal sulphide, has been used in a variety of fields owing to its metal-like electronic conductivity [12, 13], the dominant dipolar polarization and the associated relaxation phenomena [14]. The EM wave absorbing performance of CuS-based composites such as graphene $ZnFe_2O_4$@RGO@CuS [15], CuS/PANI [16], CuS/RGO/PANI/Fe_3O_4 [17], and Fe_3O_4/CuS [14], have been explored. Due to the dielectric characteristic, a combination of CuS and other absorption materials can obtain higher absorption performance.

It should be noted that the introduction of dispersed ferrites into the polymer matrix leads to an increase in the absorption of EM wave due to the influence of interphase interactions on the processes of structure formation [18]. The use of a polymer matrix makes it possible to combine the advantages of both polychlorotrifluoroethylene (flexibility, resistance to mechanical and chemical influences) and properties of functional fillers [19].

The aim of the paper was the synthesis and study the electrophysical and magnetic properties in matrix-dispersed filled systems based on polychlorotrifluorethylene (PCTFE) and modified nickel ferrite by copper sulphide.

2. EXPERIMENTAL

The sol-gel autocombustion method was used to synthesize nickel ferrite nanoparticles [20]. Iron nitrate $Fe(NO_3)_3 \cdot 9H_2O$ (pure grade), nickel nitrate $Ni(NO_3)_2 \cdot 6H_2O$ (pure grade) in molar ratio 2:1 were dissolved in deionized water (DI). Further, citric acid was added to the mixture of metal nitrates in a molar ratio of 1:1. The solution was continuously stirred using a magnetic agitator. 25% ammonia solution (0.1 M) was used to adjust the pH of the solution to 7. A viscous gel from the reaction mixture was formed at a temperature of 100°C during its constant stirring. Upon further heating, the gel combusted in a self-propagation manner to form a brown powdery. Then, the powder was heat treated at 600°C in air for 5 h.

The synthesized nickel ferrite was dispersed in DI for 10 minutes and then it was added to the prepared aqueous of hexadecyltrimethylammonium bromide (CTAB) solution and aging for 12 hours under continuous stirring solution. CTAB was used as surfactant. Then the $NiFe_2O_4$ were washed by DI water for several times and redispersed into Na_2S aqueous solution for further use. This solution was stirred at 40°C for 3 h. Then the copper sulphate (which act as sources of Cu^{2+})

aqueous solution was added dropwise into the above Na_2S aqueous solution and stirred for 3 h. Finally, the samples were centrifuged, washed several times with deionized water and ethanol, and then dried for 12 h at 60°C. The concentration of copper sulphide on a surface of ferrite was 0.2 and 0.42 volume fractions.

Powders of modified ferrite and polymer were mixed mechanically and ground in an agate mortar. Thereafter, the mixture of powders was compressed with a pressure of 2 MPa at a polymer melting temperature of 240°C to obtain $CuS/NiFe_2O_4$–PCTFE composites.

A microwave interferometer for measuring the phase velocity of EM waves in composite materials was assembled using commercial devices. A simplified block diagram is shown in Fig. 1. The method consists in measuring the amplitude and the phase of the electromagnetic wave passing through the material [21].

The calculation of ε' and ε'' was carried out using the obtained experimental values of attenuation (A_t) when the EM wave passes through the sample, the phase change $\Delta\varphi$ EM wave and the standing wave ratio (S). The reflection coefficient (R) of EM wave from the material is given according to equation

$$R = \frac{(S-1)^2}{(S+1)^2}. \tag{1}$$

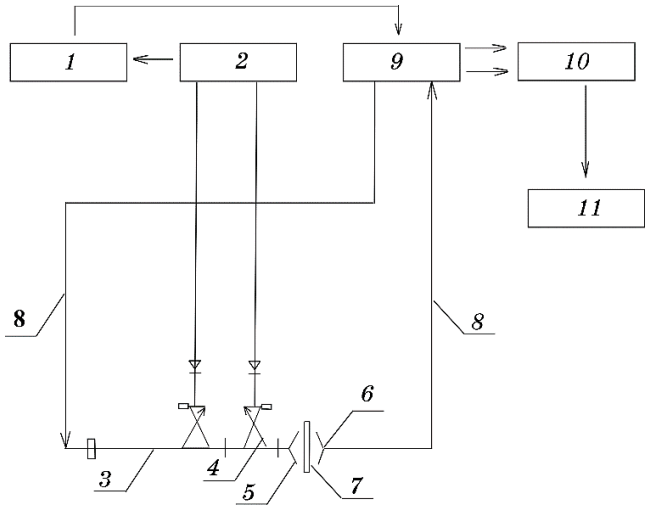

Fig. 1. The block diagram of the experimental setup for measurement the complex permittivity: 1—microwave generator, 2—indicator block of the voltage standing wave ratio, 3, 4—an ordinary broad-wall waveguide directional coupler, 5, 6—the transmitting and receiving antennas, 7—sample, 8—microwave paths, 9—phase meters (RFK2-18), 10—analog-to-digital converter, 11—computer.

EM wave absorption (A) by material is given by

$$A = A_t - R. \tag{2}$$

The real (ε') and imaginary (ε'') components of the complex permittivity were determined by the real (k') and imaginary (k'') parts of the complex wave number for a given frequency (ω) as follows:

$$\varepsilon' = \left(\frac{c}{\omega}\right)^2 \left(k'^2 - k''^2\right), \tag{3}$$

$$\varepsilon'' = 2k'k''\left(\frac{c}{\omega}\right)^2, \tag{4}$$

where c is the speed of light in vacuum.

Equations for the indexes k' and k'' can be obtained by determining the modulus of vector addition of two interfering waves of the measuring and reference paths:

$$k' = \frac{\omega}{c} + \frac{\Delta\phi}{d}, \tag{5}$$

$$k'' = \frac{0.5\ln(A_t - R)}{d}, \tag{6}$$

where d is sample thickness.

The formula for loss tangent is

$$\mathrm{tg}\delta = \frac{\varepsilon''}{\varepsilon'}. \tag{7}$$

The experimental error did not exceed 5%.

The immittance meter (E7-14, USSR) was used to determine the parameters of conductivity (σ) of composites by two-contact method [22]. These measurements were carried out at low frequency (100 Hz).

Crystalline structure of the samples was characterized by x-ray diffractometer DRON-4-07 (Lomo, USSR) with CoK_α radiation. Scherrer's equation (Eq. (8)) [23] was used to determine the crystal sizes of the samples from the width of the most intense line in XRD patterns.

$$D = \frac{0.9\lambda}{\beta\cos\theta}. \tag{8}$$

where λ is the x-ray wavelength (0.1789 nm), θ is the Bragg diffraction angle, β is the full width at half maxima of the peak [24].

Information about the morphologies and microstructures of composites was determined using transmission electron microscope (TEM)

(JEOL-1200 EX, Jeol, Japan) images of the as-synthesized products.

Magnetic properties for synthesized materials were investigated using a vibrating sample magnetometer [25, 26].

3. RESULTS AND DISCUSSION

The TEM images of the synthesized ferrite nanoparticles $NiFe_2O_4$ and nanocomposites $CuS/NiFe_2O_4$ are presented in Fig. 2. Partially agglomerated and individual particles are found in all images. The results of a TEM study indicated that nanoparticles of nickel ferrite were a size of about 60 nm (Fig. 2, *a*). Smaller nanoparticles (~15–20 nm) in TEM images (Fig. 2, *b*–*d*) after modification of nickel ferrite with copper sulphide were observed probably correspond to CuS.

The results of an x-ray diffraction study shown that the main reflections synthesized ferrite corresponded to the cubic structure of $NiFe_2O_4$ (JCPDS No. 86-2267) (Fig. 3, curve *1*) and to the (111), (220), (311), (222), (400), (422), (511), (440) crystalline planes. The size of the $NiFe_2O_4$ crystallites was 35 nm. Additional reflections also were observed. These reflections corresponded to the hexagonal structure of Fe_2O_3 (JCPDS 33-664), which was formed after extended annealing the ferrite sample in air at 650°C. Cubic phase CuS (JCPDS 75-2235) corresponded to reflections on diffraction curves (Fig 3, curve *2, 3*) for nickel ferrites modified with copper sulphide. The crystallite sizes of copper sulphide for all samples were 22–25 nm.

Figure 4 shows the TG/DTA thermograms of synthesized ferrite and nanocomposites $CuS/NiFe_2O_4$ recorded between 25 and 1000°C. The TG/DTA thermograms of nickel ferrite sample showed weight loss of about 6.5% in the temperature range 25–950°C due to of desorption water from the sample surface (Fig. 4, curves *1a*, *1b*). The obtained results confirm the formation of a stable crystal structure of ferrite at an annealing temperature of 650°C for 5 hours. For ferrite samples modified with copper sulphide, as a result of transformations $CuS \rightarrow CuO$ with an increase of temperature to 800°C, a weight loss of up to 32% was observed (Fig. 4, curves *2a*, *3b*) [27]. It should be noted that the character of the TG and DTA curves for the modified samples ($CuS/NiFe_2O_4$) changed symbiotically. There are four stages of thermal decomposition of copper sulphide [28]:

– CuS was converted into $Cu_{1.8}S$ and Cu_2S due to the release of sulphur and its oxidation to SO_2 (290°C–320°C);

– oxidation of sulphides: to copper oxides (Cu_2O and CuO (can also be formed by oxidation of Cu_2O)) or to copper sulphates (Cu_2SO_4, $CuSO_4$ (formed by direct oxidation of Cu_2O or by reaction between the released SO_2 and Cu_2O) (345°C–400°C);

– the formation of oxysulphides ($CuSO_4$ and CuO, $CuSO_4$) as a result of the reaction between copper oxide, oxygen and released SO_2 (322°C–

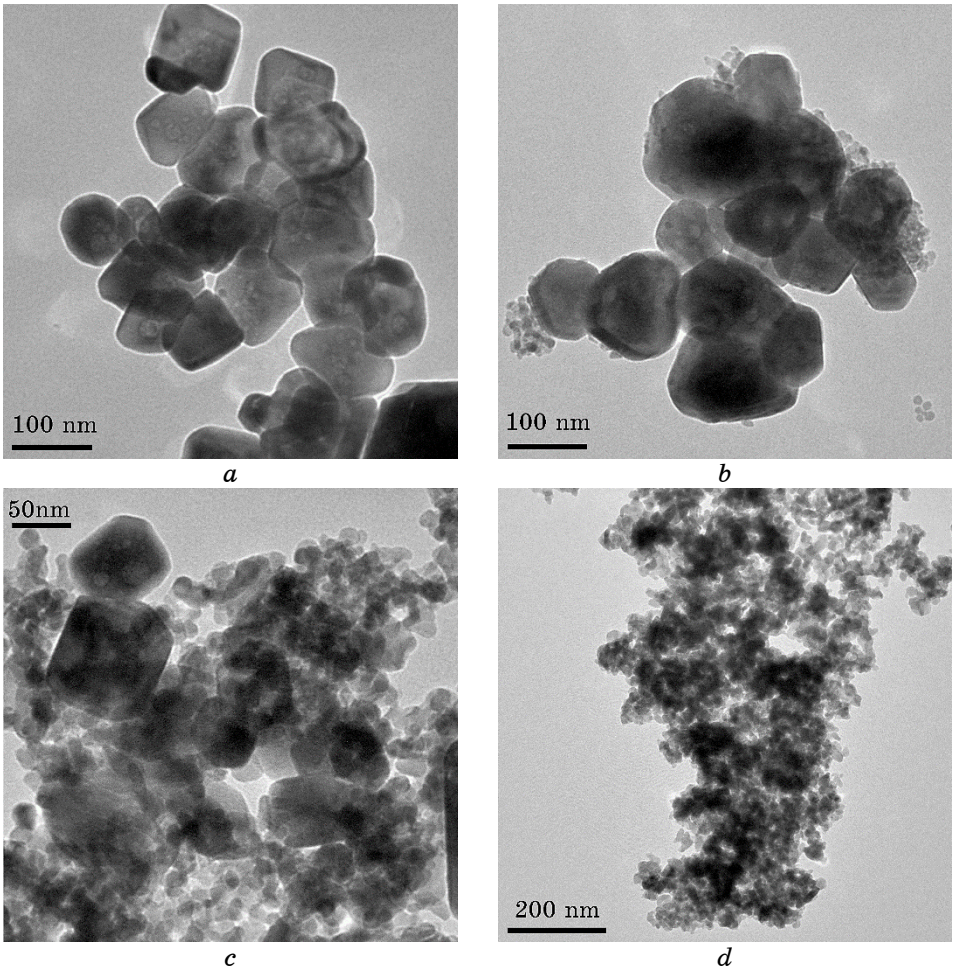

Fig. 2. TEM images of synthesized ferrites and corresponding modified ferrites *a*—$NiFe_2O_4$, *b*—$0.2CuS/NiFe_2O_4$, *c*—$0.38CuS/NiFe_2O_4$, *d*—$0.42CuS/NiFe_2O_4$.

584°C);

– decomposition of oxysulphates with the subsequent formation of CuO (608°C–783°C).

A shift of the DTA peaks (Fig. 4, curves *2b*, *3b*) to higher temperatures with an increase in the volume content of copper sulphide in the modified samples was observed. It is known that the particle size affects the intensity and shift of the peaks of endo- and exothermic effects [29]. With a decrease in the particle size, the intensity of the thermoanalytical curves decreases with a simultaneous shift of reflections to the region of low temperatures. From the TEM images data

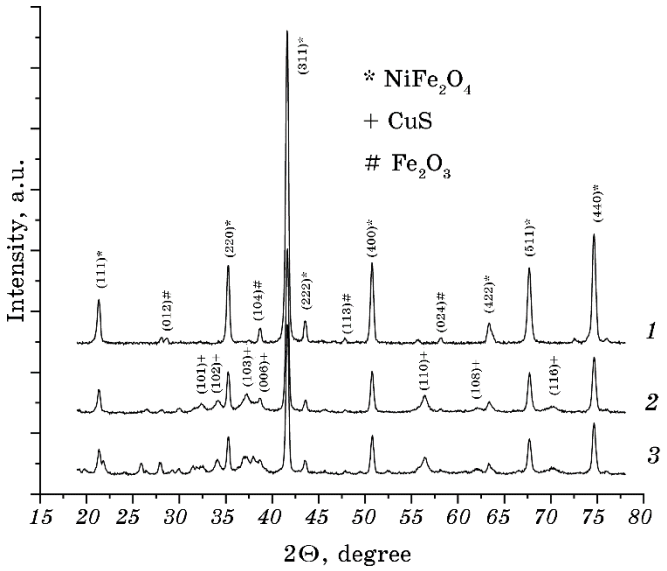

Fig. 3. X-ray diffraction patterns of synthesized samples: *1*—$NiFe_2O_4$, *2*—$0.38CuS/NiFe_2O_4$, *3*—$0.42CuS/NiFe_2O_4$.

(Fig. 2), different sizes of CuS particles on the $NiFe_2O_4$ surface with a change in the volume content of the components in the composites were determined.

The experimental results of the complex permittivity for the system $CuS/NiFe_2O_4$ are presented in Fig. 5. The nonlinear character of the increase of the values of ε', ε'' in three-component systems with an increase of the volume content of the conducting component was observed. Well-separated clusters of copper sulphide are formed on the surface of nickel ferrite during the growth of CuS particles with a concentration below 0.38. If the concentration of copper sulphide is higher than 0.38, more branched clusters are observed (Fig. 2, *c*, *d*). The formation of a layer of copper sulphide on the surface of the ferrite is similar to the formation of electrically conductive spheres. It is known that an EM wave penetrates the conductive material to the skin depth [30]. Specific absorption of EM radiation is more effective using hollow conductive balls. It is shown that the highest values of the complex permittivity are obtained for polymer composites $0.32CuS/NiFe_2O_4$ and $0.42CuS/NiFe_2O_4$. The high values ε' and ε'' conditioned by the peculiarities of structuring $CuS/NiFe_2O_4$ in the polymer matrix and the influence of the boundary layers of the polymer on the electrophysical parameters [31].

The change in the electrophysical characteristics depending on the concentration of the conducting component was also observed for pol-

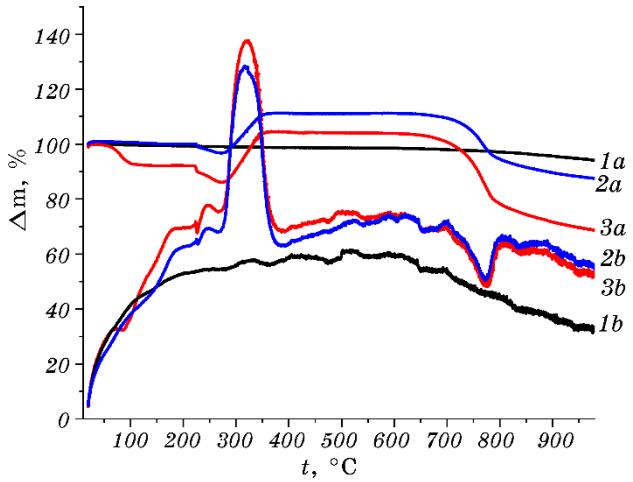

Fig. 4. Derivatograms of synthesized nanoparticles: *1*—$NiFe_2O_4$, *2*—$0.38CuS/NiFe_2O_4$, *3*—$0.42CuS/NiFe_2O_4$. (*a*—TG, *b*—DTA).

ymer composites based on modified oxides ($CuI/BaFe_{12}O_{19}$ [32], $CuI/CoFe_2O_4$, $CuI/NiFe_2O_4$ [33], CuI/MgO [34]).

The dependences of the electrical conductivity at a low frequency on the volumetric content of copper sulphide for three-component systems are shown in the Fig. 6. The electrical conductivity of polymer composites $0.38CuS/NiFe_2O_4$-PCTFE and $0.42CuS/NiFe_2O_4$–PCTFE (curves *3*, *4*) is 4–5 orders of magnitude higher than for composites with a low content of copper sulphide on the surface of nickel ferrite (curves *1*, *2*). Perhaps, this is due to a change of the sizes of copper sulphide particles or the structure of their clusters on the surface of nickel ferrite.

The conductivity results were analysed using percolation theory. According to equation (9), the values of the percolation threshold for polymer composites were calculated (Table 1).

$$\sigma = \sigma_i(\phi - \phi_c)^t, \tag{9}$$

where σ—the electrical conductivity of composite, σ_i—the electrical conductivity of the filler; ϕ—the filler volume fraction; ϕ_c—the percolation threshold, *t*—the critical exponent.

It is shown that an increase of the volume content of conductivity component in polymer composites lead to shift of the percolation threshold to the region of low concentrations of to the region of low concentrations copper sulphide.

It should be noted that for systems $0.42CuS/NiFe_2O_4$–PCTFE and $0.38CuS/NiFe_2O_4$–PCTFE, the values of electrical conductivity differ

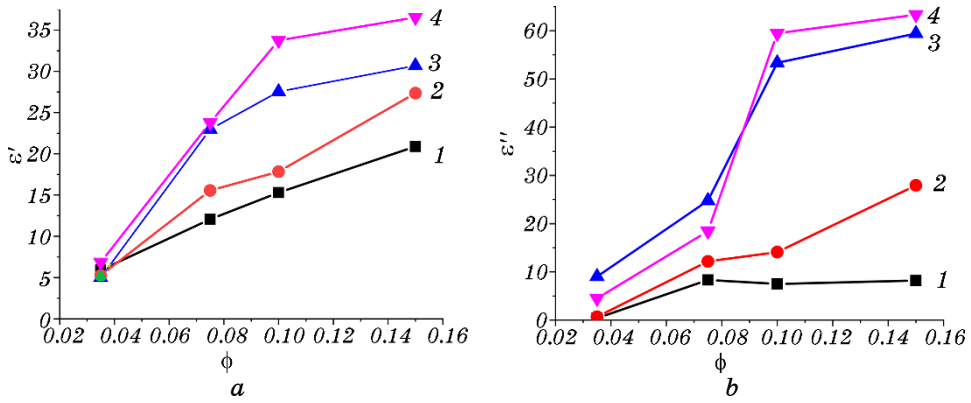

Fig. 5. Dependences of the ε′ (*a*) and ε″ (*b*) at 9 GHz of the of copper sulphide volume fractions (ϕ) in polymer composite systems *1*—0.2CuS/$NiFe_2O_4$, *2*—0.32CuS/$NiFe_2O_4$, *3*—0.38CuS/$NiFe_2O_4$, *4*—0.42CuS/$NiFe_2O_4$.

insignificantly. At such concentrations of copper sulphide, an increase in the size of CuS particles is observed on the ferrite surface. Such an increase of the size of particles has no significant effect on the formation of conducting cluster structures in the polymer.

Figure 7 shows the study of the temperature dependences of the electrical conductivity of CuS/$NiFe_2O_4$ with different contents of the conducting component. The conductivity values of the modified composites changed insignificantly with increasing temperature. At the volumetric fractions ($0.2 \le \phi \le 0.42$) of copper sulphide in CuS/$NiFe_2O_4$ system, the electrical conductivity of the nanocomposites is determined by the conductive component—copper sulphide.

The values of the real (μ′) and imaginary component (μ″) of complex permeability at 9 GHz for the synthesized nickel ferrite and it modified by copper sulphate are presented (Table 2).

The magnetization hysteresis loops CuS/$NiFe_2O_4$ composites and $NiFe_2O_4$ were obtained at room temperature (Fig. 8). With an increase of the volumetric content of copper sulphide in composites CuS/$NiFe_2O_4$, a decrease in the values of the specific saturation magnetization was observed. Magnetic characteristics for the all samples

TABLE 1. Parameters of the percolation transition of polymer composites.

Samples	ϕ_c	t
0.32CuS/$NiFe_2O_4$–PCTFE	0.996 ± 0.05	2.2 ± 0.1
0.38CuS/$NiFe_2O_4$–PCTFE	0.05 ± 0.05	1.62 ± 0.1
0.42CuS/$NiFe_2O_4$–PCTFE	0.06 ± 0.05	1.6 ± 0.1

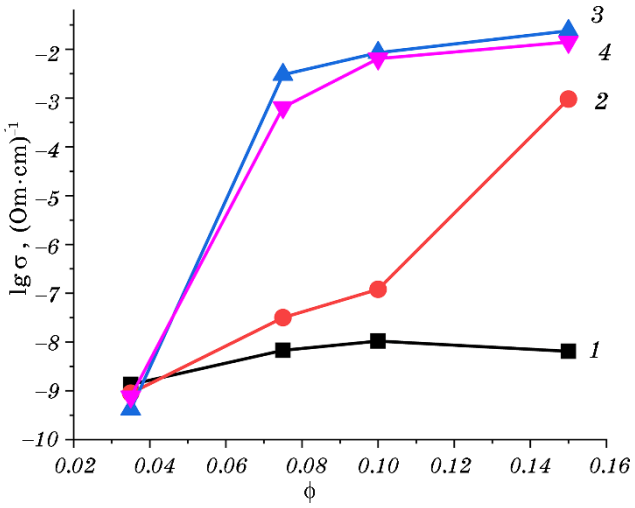

Fig. 6. Dependences of the electrical conductivity logarithms of the copper sulphide volume fractions (ϕ) in polymer composite systems at a frequency of 100 Hz: *1*—0.2CuS/$NiFe_2O_4$, *2*—0.32CuS/$NiFe_2O_4$, *3*—0.38CuS/$NiFe_2O_4$, *4*—0.42CuS/$NiFe_2O_4$.

are listed in Table 3.

The presence of a 'demagnetized' hematite layer on a ferrite particle leads to a decrease of the specific saturation magnetization. Thus, for a bulk ferrite with a particle size of ~ 60 nm, the calculated specific saturation magnetization is 58.7 G·cm^3/g, and for synthesized ferrite this value is 35.6 G·cm^3/g. The electrophysical parameters of polymer nanocomposites based on modified ferrites can be regulated due to changes in the thickness of the α-Fe_2O_3 layer on the ferrite surface during its synthesis. It should be noted that small spontaneous magnetization of the antiferromagnetic hematite in the temperature range (–27–670)°C is ~10^{-5} of the sum of the magnetizations of the sublattices [35]. The 'demagnetized' hematite layer on ferrite particles make for reduce of the total magnetic moment [36].

TABLE 2. Permeability of as-synthesized and modified ferrite.

Sample	μ′	μ′′
$NiFe_2O_4$	1.01	0.02
0.2CuS/$NiFe_2O_4$	1.05	0.03
0.32CuS/$NiFe_2O_4$	1.08	0.03
0.38CuS/$NiFe_2O_4$	1.15	0.04
0.42CuS/$NiFe_2O_4$	1.18	0.04

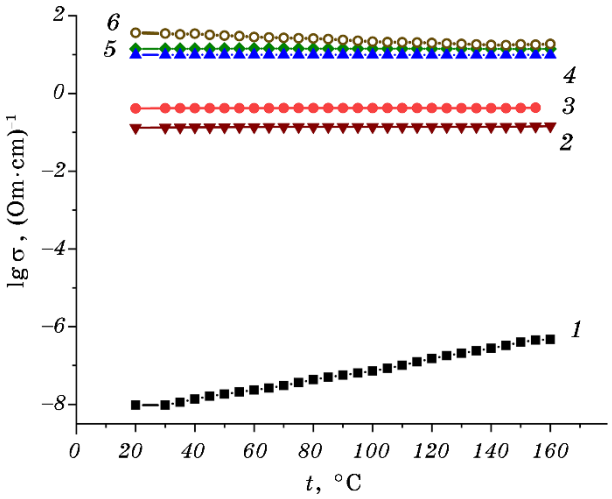

Fig. 7. Temperature dependence of the logarithm of electrical conductivity (σ) at a frequency of 100 Hz for nanocomposites $CuS/NiFe_2O_4$. Volume fractions of copper sulphide: *1*—0; *2*—0.25; *3*—0.32; *4*—0.38; *5*—0.42; *6*—1.

The core–shell model [36] was used to determine the specific saturation magnetization of a complex nanoparticle with external diameter D.

$$M_s^n = M_s^b \left[1 - \frac{2}{D_m} (h_{\alpha\text{-}Fe_2O_3} + a_0) \right]^3, \qquad (10)$$

where M_s^n—specific saturation magnetization of α-Fe_2O_3/ferrite par-

TABLE 3. Magnetic characteristics of as-synthesized ferrites and their derivatives.

Sample composition*	H_c, (Oe)	M_s (G·cm³/g)	M_r (G·cm³/g)	M_r/M_s	ϕ ($NiFe_2O_4$)
$NiFe_2O_4$	131	35.6*)	3.50	0.098	1
$0.2CuS/NiFe_2O_4$	106	31.8*)	3.26	0.102	0.89
$0.32CuS/NiFe_2O_4$	94	29.7*)	3.02	0.101	0.83
$0.38CuS/NiFe_2O_4$	107	27.9*)	2.94	0.105	0.78
$0.42CuS/NiFe_2O_4$	169	23.9*)	2.45	0.102	0.66

where H_c—coercive force, M_s—specific saturation magnetization, M_r—residual specific magnetization and M_r/M_s—relative residual specific magnetization; *—with α-Fe_2O_3 on the surface of the ferrite particles [37].

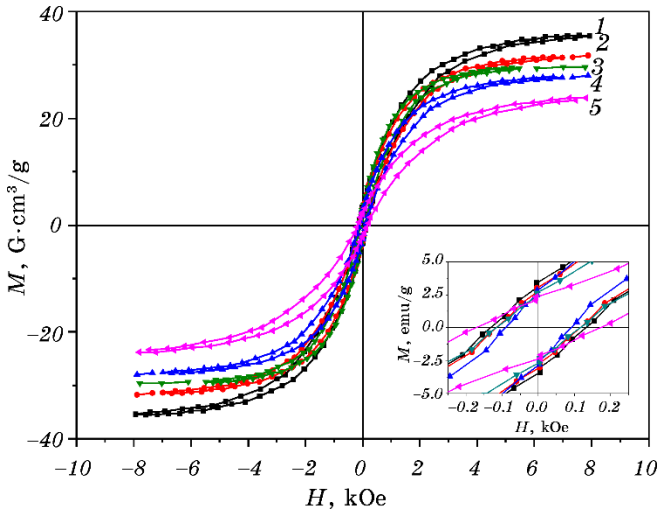

Fig. 8. Hysteresis loops and their primary areas of nanocomposites $CuS/NiFe_2O_4$. Volume fractions of copper sulphide: *1*—0; *2*—0.2; *3*—0.32; *4*—0.38; *5*—0.42.

ticle, M_s^b —specific saturation magnetization bulk ferrite, D_m—an average external diameter of particles, $h_{\alpha\text{-}Fe_2O_3}$ —layer thickness of the α-Fe_2O_3, a_0—a lattice constant of the ferrite.

The thickness of the hematite layer on the surface of $NiFe_2O_4$ calculated according to equation (10) is ~ 3.7 nm. The density of the magnetic moment of composites decreases due to the presence of copper sulphide and a hematite shell on the surface of nickel ferrite nanoparticles.

4. CONCLUSIONS

Nanosized nickel ferrite with average particles size of 60 nm was synthesized by the sol-gel autocombustion method. The surface of nickel ferrite was modified by copper sulphide with particles size of 15–20 nm. The volume fractions of copper sulphide in $CuS/NiFe_2O_4$ nanocomposites were from 0.2 to 0.42.

The electrical and magnetic properties of polymer composites based on nickel ferrite modified by copper sulphide were studied. An increase of 2–3 times in the values of ε', ε'' in the microwave range for $CuS/NiFe_2O_4$–polychlorotrifluoroethylene systems with an increase in the volume content of copper sulphide from 0.32 to 0.42 was observed. The values of electrical conductivity for the $0.2CuS/NiFe_2O_4$–PCTFE system are 4–5 orders of magnitude lower than for the $0.42CuS/NiFe_2O_4$–PCTFE system with an increase in the concentration

of copper sulphide in polymer composites. Such effects are due to the increase in the interfacial surface of the polymer and $CuS/NiFe_2O_4$, as well as the formation of more branched clusters of ferrite particles modified by copper sulphide. It is shown that the regulation of the values of the permittivity and permeability of polymer nanocomposites is achieved by modifying dispersed fillers by conductive components.

REFERENCES

1. D. Wanasinghe, F. Aslani, G. Ma, and D. Habibi, *Construction and Building Materials*, **231**: 117116 (2020).
2. M. Green and X. Chen, *Journal of Materiomics*, **5**, Iss. 4: 503 (2019).
3. L. Li, S. Liu, and L. Longfei, *J. Alloy Compd.*, **722**: 158 (2017).
4. E. Ghashghaei, S. Kheirjou, S. Asgari, and H. Kazerooni, *C. R. Chimie*, **21**, Iss. 9: 862 (2018).
5. H. Yang, T. Ye, Y. Lin, J. Zhu, and F. Wang, *J. Alloys Compd.*, **683**: 567 (2016).
6. J. Xue, H. Zhang, J. Zhao X. Ou, and Y. Ling, *J. Magn. Magn. Mat.*, **514**: 167168 (2020).
7. K. Egizbek, A.L. Kozlovskiy, K. Ludzik, M. V. Zdorovets, I. V. Korolkov, B. Marciniak, M. Jazdzewska, D. Chudoba, A. Nazarova, and R. Kontek, *Ceramics International*, **46**, Iss. 10: 16548 (2020).
8. P. Liu, Y. Huang, and X. Sun, *Mater. Lett.*, **112**: 117 (2013).
9. J. Tang, K. Wang, Y. Lu, N. Liang, X. Qin, G. Tian, D. Zhang S. Feng, and H. Yue, *J. Magn. Magn. Mat.*, **514**: 167268 (2020).
10. H. Tammareddy. K. Ramji, P. Siva Naga Sree, and B. V. S. R. N. Santhosi, *Materials Today: Proceedings*, **18**, Part 1: 420 (2019).
11. J. Liao, J. Qiu, G. Wang, R. Du, N. Tsidaeva, and W. Wang, *J. Colloid Interface Sci.*, **604**: 537 (2021).
12. Y. K. Hsu, Y. C. Chen, and Y. G. Lin, *Electrochim. Acta*, **139**: 401 (2014).
13. Y. Wang, X. Zhang, P. Chen, H. Liao, and S. Cheng, *Electrochim. Acta*, **80**: 264 (2012).
14. X. Sun, M. Sui, G. Cui, L. Li, X. Li, X. Lv, F. Wu, and G. Gu, *RSC Adv.*, **13**: 17489 (2018).
15. Y. Wang, X. Gao, X. Wu, W. Zhang, Q. Wang, and C. Luo, *Ceramics International*, **44**, Iss. 8: 9816 (2018).
16. J. Sun, Y. Shen, and X.-S. Hu, *Polym. Bull.*, **75**: 653 (2018).
17. Y. Wang, X. Gao, W. Zhang, C. Luo, L. Zhang, and P. Xue, *J. Alloys Compd.*, **757**: 372 (2018).
18. R. S. Yadav, I. Kuritka, J. Vilcáková, M. Machovský, D. Škoda, P. Urbánek, M. Masar, M. Goralik, M. Urbánek, L. Kalina, and J. Havlica, *Nanomaterials*, **9**, Iss. 4: 621 (2019).
19. S. Ebnesajjad, *Fluoroplastics Volume 1: Non-Melt Processible Fluoropolymers—The Definitive User's Guide and Data Book* (2nd Edition, eBook ISBN: 9781455732005 William Andrew Publishing: 2015), p. 718.
20. B. Xu, T. Ding, Y. Zhang, Y. Wen, Z. Yang, and M. Zhang, *Mater. Lett.*, **187**: 123 (2017).
21. L. N. Ganiuk, V. D. Ignatkov, S. N. Makhno, and P. N. Soroka, *Ukr. Phys. J.*, **40**: 627 (1995) (in Russian).

22. L. P. Pavlov, *Methods for Measuring the Parameters of Semiconductor Materials* (Moscow: Vysshaya Shkola: 1987) (in Russian).
23. A. Guinier, *Rentgenografiya Kristallov* [X-ray Crystallography] (Moscow: Gos. Izd-vo Fiz.-Mat. Lit: 1961) (in Russian).
24. P. Scardi, M. Leoni, and R. Delhez, *J. Appl. Crystallogr.*, **37**: 381 (2004).
25. S. Foner, *Rev. Sci. Instrum.*, **30**: 548 (1959).
26. A. L. Petranovska, N. V. Abramov, S. P. Turanska, P. P. Gorbyk, A. N. Kaminskiy, and N. V. Kusyak, *J. Nanostruct. Chem.*, **5**: 275 (2015).
27. J. G. Dunn and C. Muzenda, *Thermochimica Acta*, **369**: 117 (2001).
28. C. M. Simonescu, V. S. Teodorescu, O. Carp, L. Patron, and C. Capatina, *J. Therm. Anal. Calorim.*, **88**, Iss. 1: 71 (2007).
29. N. D. Topor, L. P. Ogorodova, and L. V. Melchakova, *Thermal Analysis of Minerals and Inorganic Compounds* (Moscow: Publishing house of Moscow State University: 1987) (in Russian).
30. E. I. Nefyodov and S. M. Smolskiy, *Understanding of Electrodynamics, Radio Wave Propagation and Antennas* (Scientific Research Publishing: Inc. USA: 2013).
31. Y. Mamunya, L. Matzui, L. Vovchenko, O. Maruzhenko, V. Oliynyk, S. Pusz, B. Kumanek, and U. Szeluga, *Composites Science and Technology*, **170**: 51 (2019).
32. R. V. Mazurenko, S. L. Prokopenko, M. V. Abramov, G. M. Gunja, S. M. Makhno, and P. P. Gorbyk, *Nanosistemi, Nanomateriali, Nanotehnologii*, **19**, No. 1: 111 (2021).
33. S. L. Prokopenko, R. V. Mazurenko, G. M. Gunja, N. V. Abramov, S. M. Makhno, and P. P. Gorbyk, *J. Magn. Magn. Mat.*, **494**: 165824 (2020).
34. R. V. Mazurenko, P. P. Gorbik, G. M. Gunya, and S. N. Makhno, *Physics and Chemistry of Solid State*, **17**, No. 4: 482 (2016).
35. R. D. Zysler, M. Vasquez-Mansilla, C. Arciprete, M. Dimitrijewits, D. Rodriguez-Sierra, and C. Saragovi, *J. Magn. Magn. Mat.*, **224**: 39 (2001).
36. N. V. Abramov, S. P. Turanska, A. P. Kusyak, A. L. Petranovska, and P. P. Gorbyk, *J. Nanostruct. Chem.*, **6**: 223 (2016).
37. L. Lv, J.-P. Zhou, Q. Liu, G. Zhu, X.-Z. Chen, X.-B. Bian, and P. Liu, *Phys. E: Low-Dimens. Syst. Nanostructures*, **43**, Iss. 10: 1798 (2011).